EPR spectroscopy of the radical–molecular complex NH$_2$–HF formed in low temperature chemical reaction of fluorine atoms with NH$_3$ molecules trapped in solid argon

I.U. Goldschleger, A.V. Akimov, E.Ya. Misochko[*]

Institute of Problems of Chemical Physics of the Russian Academy of Sciences, Chernogolovka, Moscow Region, 142432, Russia

Abstract

Chemical reactions of F atoms with NH$_3$ molecules in a solid argon matrix were studied with electron paramagnetic resonance (EPR) spectroscopy. Fluorine atoms were generated by UV photolysis of F$_2$ molecules in dilute solutions of F$_2$ and NH$_3$ in solid Ar. To distinguish reactions of photogenerated translationally excited F atoms (at 15 K) from reactions of diffusing thermal F atoms (at $T > 20$ K) experiments were conducted at different temperatures. The radical–molecular complex NH$_2$–HF is observed for the first time as an intermediate product in reactions involving both types of F atoms. The hyperfine (hf) constants of the NH$_2$–HF complex: $a_N = 1.20$ mT, $a_H = 2.40$ mT, and $a_F = 0.70$ mT, were determined from analysis of EPR spectra in isotopic substituted samples (^{14}N $\rightarrow$ ^{15}N, and H $\rightarrow$ D). The performed calculations revealed that complex NH$_2$–HF has a planar C$_{2v}$ structure and a binding energy of 12.3 kcal/mol. Optimisation of arrangement of the complex in an argon lattice shows that the complex suffers a minor distortion in crystalline lattice relative to its equilibrium geometry in a gas phase. Calculated hf constants of the complex are in good agreement with those observed in EPR experiments. © 2000 Elsevier Science B.V. All rights reserved.

Keywords: Radical–molecular complexes; EPR spectroscopy; Solid-state chemical reactions

1. Introduction

Long-lived intermediate complexes formed in the vicinity of the transition state of atom–molecular chemical reactions appear to play a significant role in reaction dynamics. Dynamics of these complexes govern the energy distributions and fly apart angles of products. To have a comprehensive description of the reaction, it is indispensable to know the geometry and eigen frequencies of intermediates in their evolution in the interaction region.

Investigation of geometry and dynamics of intermediates constitutes one of the most active research fields nowadays. Although time-resolved methods are in progress to access this part of potential energy surface of elementary chemical reactions in a gas phase (see for the example Refs. [1,2]), the methods of low-temperature spectroscopy of isolated intermediates continue to play a significant role due to their universality and reliability in interpretation of experimental data.

Recently we have proposed a high resolved electron paramagnetic resonance (EPR) technique in rare gas matrices to study radical–molecular complexes R–HF, being intermediate states of gas phase

* Corresponding author. Fax: + 7-96-576-4009.
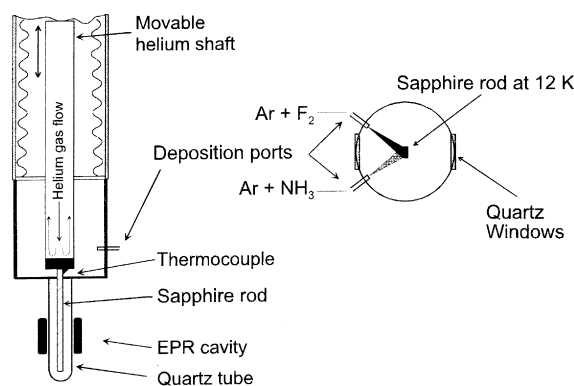*E-mail address:* misochko@icp.ac.ru (E.Ya. Misochko).

Fig. 1. Schematic drawing of the EPR cryostat and the sample deposition geometry.

reactions of fluorine atoms with small polyatomic molecules [3–5]:

$$F + RH \rightarrow HF + R \qquad (RH = H_2, CH_4) \qquad (1)$$

This methodology is based on widely used matrix isolation techniques and the high mobility of fluorine atoms in solid argon observed by Apkarian et al. [6]. It was shown that translationally excited "hot" fluorine atoms formed by UV photolysis of F_2 molecules migrate through several lattice periods [6,7]. The next unusual characteristic of F atoms is their ability to undergo thermally activated diffusion in solid argon at temperatures above 20 K. These features of "hot" and thermal fluorine atoms enable the study of reactions with various molecules imbedded in an Ar matrix. Yet, the crystalline environment prevents reaction products from flying apart and promotes fast relaxation of excess energy released in the reaction. Therefore, intermediates, which are not observable in gas phase studies, are frozen in a matrix [8]. They can then be studied with various spectroscopy techniques.

Two facts drastically diminish the inhomogeneous broadening of EPR spectra: zero nuclear spin of Ar and homogeneous distribution of the complexes $[R–HF] \leq 10^{16}$ cm^{-3} in the sample. Resolution of up to 0.01–0.05 mT is achieved. Measurement with this spectral resolution allows one to determine the total set of hyperfine (hf) constants. The hf interaction of unpaired electron with magnetic nuclei in the radical–molecular complex is very sensitive to the distance between the radical R and the HF molecule

and to their mutual orientation. Therefore, geometry of the complex could be determined by comparison of the measured hf constants with those obtained in quantum chemical calculations.

In the present research, we have used the proposed methodology to study the reaction of F atoms with NH_3 molecules isolated in an argon matrix. The original interest in studying the reaction:

$$F + NH_3 \rightarrow HF(v') + NH_2; \qquad (2)$$
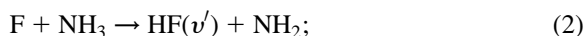
$$\Delta H_0^0 \approx -31 \text{ kcal/mol}$$

was motivated by attempts to use it as a source for chemical laser [9]. Usually, reactions of H atom abstraction from small polyatomic molecules yield extensive inverse HF internal excitation [10]. However, the attempts to obtain an inverse HF excitation in the reaction (2) were unsuccessful, despite its high exothermicity [11,12]. It was assumed that the reason was formation of long-lived FNH_3 species during the reaction. The existence of such an intermediate complex could cause randomisation of the exoergicity among its internal modes.

Ab initio calculations performed by Goddard et al. predicted $NH_2–HF$ complex formation in the exit channel of reaction (2) with the binding energy ~10 kcal/mol [13]. In the early infrared spectroscopic study of solid ternary mixtures $Ar/F_2/NH_3$, Andrews and Lascola observed the molecular complex $NH_2F–HF$. This complex was formed upon photolysis in a cage reaction at 12 K [14]:

$$[NH_3–F_2] \overset{h\nu}{\rightarrow} [NH_2F–HF] \qquad (3)$$

In this study, we have observed the radical–molecular complex $NH_2–HF$ formed in reaction (2), and measured its hyperfine (hf) constants for the first time. Comparison of the observed hf constants with those obtained from calculation shows that the structure of the complex is close to the one predicted by Goddard et al. [13]. The influence of crystalline environment on structure of the stabilised $NH_2–HF$ complexes is discussed.

2. Experimental details

Samples were prepared by co-deposition of two effusive beams (Ar:NH_3 and Ar:F_2) onto a substrate
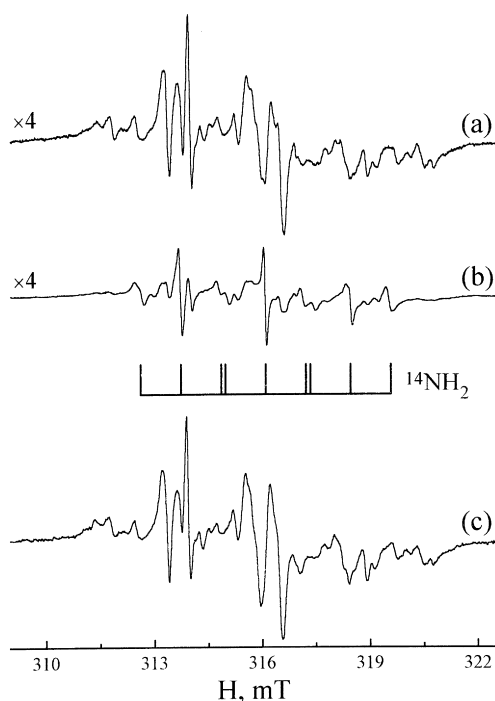
Fig. 2. EPR spectra of the Ar : F_2 : NH_3 = 1000 : 1 : 1 sample: (a) after exhaustive photolysis at 15 K; (b) after subsequent cooling to 7.7 K; (c) after annealing of the photolysed sample for 30 min at 25 K and subsequent lowering the temperature to 15 K. Intensities of the spectra are corrected in accordance with the Curie law.

cooled to 13 K. The matrix substance Ar (99.9995%) and fluorine F_2 (99.9%) were used without purification. Ammonia $^{14}NH_3$ ($^{14}NH_3$) was used after drying over NaOH. ND_3 was prepared by repeated exchange of NH_3 with D_2O followed by distillation and drying over NaOD. The deuterium purity was estimated at 90%. The sample composition was typically Ar : F_2 : NH_3 = 1000 : 1 : 1. The experiments were carried out with a home-made helium flow cryostat with a movable helium shaft (see Fig. 1). Gases were deposited from two spatially separated ports onto a flat sapphire rod ($2 \times 4 \times 50$ mm^3; deposition area was 4×5 mm^2). To minimise the probability of gas phase reactions, deposited beams were crossed only near the substrate. After deposition, the sapphire rod with the sample was lowered into the microwave cavity of the spectrometer. The temperature of the sample was measured with a thermocouple attached to the top of the rod. It was calibrated with another thermocouple attached at the sample position in sepa-

rate experiments. Calibrations showed that the temperature difference between the two ends of the rod did not exceed 0.3 K [4]. The temperature stability was 0.1 K over the range 7.7–30 K.

Fluorine atoms were generated by F_2 photolysis at $\lambda = 337$ nm with a pulsed N_2-laser (repetition frequency 1000 Hz). The average laser power did not exceed 20 mW/cm^2. Photodissociation of F_2 at these wavelengths yields two translationally excited F atoms with ~1 eV excess kinetic energy per atom. Fluorine atoms undergo thermally activated diffusion in solid argon at temperatures above 20 K. They are effectively immobilised at $T < 20$ K [6]. To distinguish the chemical reactions involving photogenerated "hot" F atoms and diffusing thermal F atoms, photolysis of F_2 molecules was performed at 15 K.

3. Results and discussion

3.1. Photolysis of Ar–F_2–NH_3 mixtures at 15 K

EPR spectra of freshly prepared samples exhibit no lines due to paramagnetic species. Short-term photolysis (~5 min) of the samples Ar : F_2 : NH_3 = 1000 : 1 : 1 at 15 K leads to appearance of the complex anisotropic spectrum. Growth of intensity of EPR lines is proportional to the time of photolysis in the initial stage, and reaches limiting values under extensive photolysis (~100 min). The EPR spectrum of reaction products after photolysis at 15 K is shown in Fig. 2(a). Lowering the temperature of the photolysed sample causes a broadening of the most of anisotropic lines, and practically, only nine lines remain in the spectrum at 7.7 K (see Fig. 2(b)). Temperature changes of the lines shape are reversible in the region 7.7–18 K. The integrated intensity of the spectrum (I_s) obeys the Curie law ($I_s \propto 1/T$). Therefore concentration of radicals does not change after completion of photolysis, and the resulting spectra correspond to superimposition of spectra of two products, at least. Furthermore, lines shape of one of them exhibits a strong reversible temperature dependent broadening, whereas lines shape of the other is exposed to weak temperature changes. Nine lines of this radical are well resolved at 7.7 K. Its spectrum shown in Fig. 2(b) corresponds to two triplet groups with hf splitting 1.05 and 2.40 mT, and $g = 2.0058$.
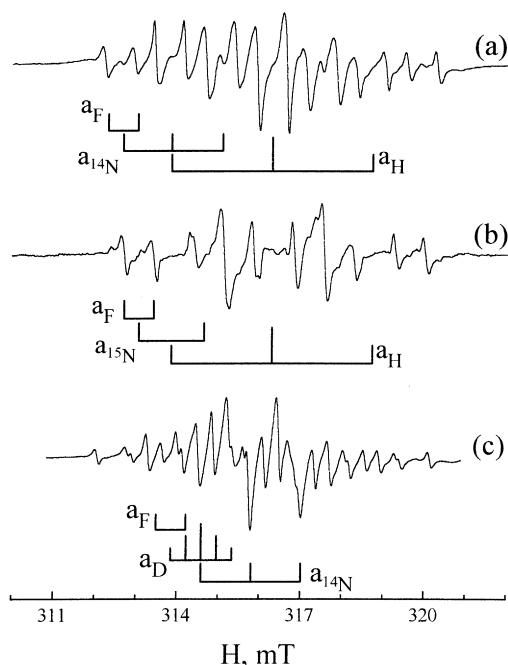
Fig. 3. EPR spectra of the samples after photolysis at 15 K and subsequent annealing at 25 K: (a) Ar/^{14}NH$_3$/F$_2$; (b) Ar/^{15}NH$_3$/F$_2$; (c) Ar/^{14}ND$_3$/F$_2$. All spectra are recorded at 35 K. (The isotopic substituted ammonia ^{14}ND$_3$ used in the experiments contains ~10% of ^{14}NH$_3$. Therefore weak outer lines in this spectrum correspond to those of the complex ^{14}NH$_2$–HF).

Both hf constants and *g*-factor are in good agreement with the data of Cochran et al. obtained for the radical NH$_2$ in solid Ar [15].

It allows us to conclude, that one of the photolysis products is the radical NH$_2$, which is formed in reaction (2) of photogenerated "hot" F atom with NH$_3$ molecule.

3.2. Annealing of the samples Ar–F$_2$–NH$_3$ photolysed at 15 K

To initiate reactions of thermal F atoms, we have performed annealing of photolysed samples at $T > 20$ K. EPR spectrum after annealing of the sample at 15 K is shown in Fig. 2(c). Annealing results in growth of its integrated intensity by a factor of 4.2. Comparison of the spectra before (Fig. 2(a)) and after (Fig. 2(c)) annealing shows that concentration of the NH$_2$ radicals does not change, while the intensity of lines of the other radical is increased four

times due to reaction of diffusing F atoms. Upon heating above 30 K, lines of this radical become narrow and isotropic. The EPR spectrum at 35 K is shown in Fig. 3(a). It consists of 14 narrow lines with a linewidth of 0.1 mT. The spectrum corresponds to three hf splitting the triplet 1:1:1 with $a_1 = 1.20$ mT, the triplet 1:2:1 with $a_2 = 2.40$ mT, and the doublet $a_3 = 0.70$ mT. Because $a_2 \approx 2 \times a_1$, four lines are compound. Thus, only 14 lines are resolved in the spectrum, instead of 18 lines corresponding to such assignment. Two triplet splittings, a_1 and a_2, are close to those for the NH$_2$ radical. Let us assume that additional doublet splitting a_3 occurs because of magnetic interaction with one of the magnetic nuclei of the HF molecule in the complex NH$_2$–HF. In order to distinguish the hf constants of magnetic H, F and N nuclei, we performed a series of similar experiments with isotopic substituted NH$_3$.

3.3. Annealing of the samples Ar–F$_2$–^{15}NH$_3$ and Ar–F$_2$–^{14}NH$_3$ND$_3$ photolysed at 15 K

EPR spectra obtained in the photolysed F$_2$/^{15}NH$_3$/Ar and F$_2$/ND$_3$/Ar samples are shown in Fig. 3(b) and (c), respectively. Referring to Fig. 3(b), the isotopic substitution of nitrogen atom, ^{14}N($J = 1$) → ^{15}N($J = 1/2$), leads to the replacement of the triplet $a_N(^{14}$N) = 1.20 mT by the doublet $a_N(^{15}$N) = 1.55 mT. Two other splittings, 2.4 and 0.70 mT, remain the same. In samples Ar–F$_2$–^{14}ND$_3$, only the triplet $a_H = 2.40$ mT is replaced by the quintet $a_D = 0.37$ mT. These findings allow to assign the hf constants a_1 and a_2 to the NH$_2$-group quite definitely. At the same time, the last doublet splitting $a_3 = 0.70$ mT (which is unchanged by isotopic substitutions mentioned above) is necessary to attribute to the ^{19}F atom, because it is the only atom having the magnetic nucleus $J = 1/2$ left in the given system. Since NH$_2$F is a closed-shell molecule, we can attribute the considered EPR spectrum to the radical-molecular complex NH$_2$–HF, assuming that the hf constant at the H atom of HF molecule a_H is less than 0.05 mT.

Based on the given analysis of EPR spectra we may conclude that reactions of photogenerated "hot" F atoms (2) produce two types of products: NH$_2$–HF complexes and spatial separated free radicals NH$_2$ and HF molecules. Comparison of

the integrated intensities of the EPR spectra shows, that the part of the complexes in total product balance equals $\eta \approx 0.85$. A much higher part of the complexes is produced in reactions of diffusing thermal F atoms at $T > 20$ K, $\eta > 0.95$. In contrast, as it was elucidated in the previous papers [3–5], the radical–molecular complexes CH$_3$–HF (binding energy ~ 2 kcal/mol) and H–HF (binding energy ≤ 100 cal/mol) did not form in reactions of "hot" F atoms with CH$_4$ and H$_2$ molecules in solid argon, and the fraction of these complexes produced in reactions of diffusing thermal F atoms did not exceed 0.6. Thus, high yield of NH$_2$–HF complexes in reactions of "hot" and thermal F atoms with NH$_3$ molecules could arise from much higher binding energy in this complex.

Therefore, the radical–molecular complex NH$_2$–HF is the main product of the reaction of mobile fluorine atoms with NH$_3$ molecules in solid Ar:

$$F + NH_3 \rightarrow NH_2\text{–}HF \tag{4}$$

3.4. Geometry optimisation of NH$_2$–HF complex

We carried out quantum chemical calculations in order to clarify the structure of the NH$_2$–HF complex. All of the computations were performed using GAUSSIAN 94 suite of codes [16] in the Institute of Organic Chemistry RAS within grant RFBR no. 98-07-90290. A density functional method B3LYP with EPR-3 (of triple ξ plus double polarisation quality) basis set [17] was used for geometry optimisation and calculation of hf constants. In preliminary calculations we were convinced that this method reproduced the hf constants a_N and a_H in NH$_2$ free radical with accuracies 0.01 and 0.1 mT relative to the values determined by the experiment, respectively.

The NH$_2$–HF complex has a planar C$_{2v}$ structure, which is similar to that calculated earlier by Goddard et al. [13]. The binding energy of the complex is equal to 12.3 kcal/mol. The equilibrium structure and both experimental and theoretically calculated isotropic hf constants of the NH$_2$–HF complex are given in the

scheme:
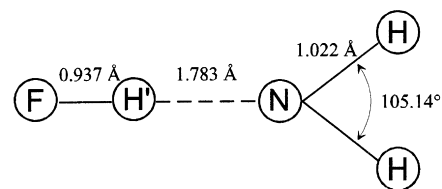
a(calc), mT	-0.70	0.02	1.15	-2.30
a(exp), mT	-0.70	<0.05	1.20	-2.40

$$\text{(5)}$$

Calculated hf constants a_N, a_H and a_F are in good agreement with the experimental data. Yet, the hf constant at the proton of the HF molecule a_H is less than 0.05 mT and, as was noticed above, such splitting cannot be resolved at the given experimental conditions.

It should be noted that the isotropic hf constant at the H atom of the HF molecule a_H in the CH$_3$–HF [4], H–HF [5], and NH$_2$–HF complexes is much less than a_F, $a_F \gg a_H$. Isotropic hf constant a_n is related to the spin-densities $\rho(\mathbf{r}_n)$ at the corresponding nuclei by

$$a_n = \frac{8\pi}{3} g_e \beta_e g_n \beta_n \rho(\mathbf{r}_n) \tag{6}$$

where g_n and β_n are the nuclear g-factor and nuclear magneton, respectively. The term g_e is the g value of the electron and β_e is the Bohr magneton. As $g_F \beta_F \approx g_H \beta_H$ and $a_F \gg a_H$ for nuclei of the HF molecule in the complex, the spin-density at the ^{19}F nucleus is much higher than that at the H atom. This peculiarity seems to be general for all studied radical–molecular complexes CH$_3$–HF, H–HF and NH$_2$–HF.

As listed above the binding energy of CH$_3$–HF and H–HF complexes is equal to 2 and 0.1 kcal/mol, respectively. These complexes are weakly bound, while the NH$_2$–HF complex could be assigned to the medium strength hydrogen-bonded complex (its binding energy is 12.3 kcal/mol). As it follows from the calculated charges distribution in the complex ($q_F = -0.4683e$, $q_{H'} = 0.4174e$, $q_N = -0.3909e$, $q_H = 0.2209e$, where e is the charge of electron), the energy of electrostatic intermolecular interaction equals 3.0–3.5 kcal/mol, i.e. only $\sim 25\%$ of the binding energy. It means that NH$_2$–HF has covalent bonding character rather than ionic and the origin of

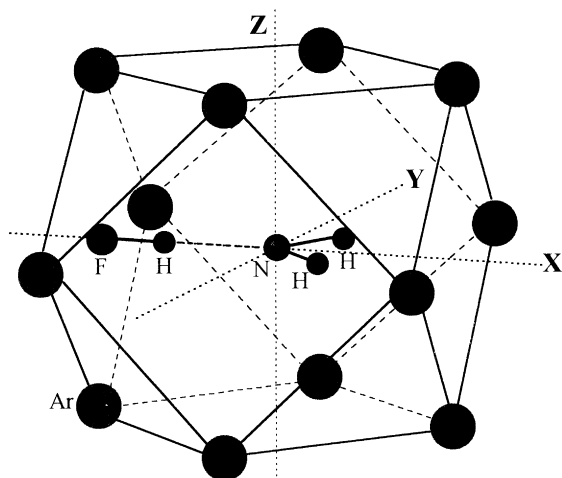Fig. 4. Arrangement of the complex NH_2–HF in argon lattice. Twelve nearest neighbour Ar atoms are shown.

bond in the complex should be similar to the NH_3–HF complex described recently by Zhang et al. [18].

3.5. Arrangement of NH_2–HF complex in an argon lattice

Starting from the calculated structure we carried out optimisation of the arrangement of NH_2–HF complex in argon lattice. As each isolated NH_3 molecule occupies a singly substitutional argon lattice site, we anticipated that the NH_2-group of the complex would also be located in the same type of site. There are only C_3 and C_4 crystal axes in the fcc argon lattice. However, the C_2 axis of the complex NH_2–HF is incompatible with the C_3 axis of a crystal. Then, as a starting orientation of the complex in a lattice, the position, in which the C_2 axis of the complex coincides with the C_4 crystal axes was used. The subsequent minimisation of the total energy of doped argon cluster was done using molecular dynamics (MD) simulation as described in Refs. [4,19]. The argon cluster contained 365 atoms, and the central atom was substituted by the complex. The 194 argon atoms on the surface of the cluster were fixed, and the motion of the remaining 171 internal atoms was described by Newton's equations of motion. Parameters of pair atom–atom potentials Ar–Ar, Ar–F, Ar–N, and Ar–H were taken from Refs. [20,21]. Initially, all of the argon atoms were

placed at the sites of undistorted lattice with zero velocities. The MD simulation was stopped whenever the kinetic energy of the dynamically evolving system reached a maximum. At this point, the kinetic energy of the system was rest to zero, and the next evolution cycle was started. The simulation was stopped if no further increase of kinetic energy occurred, i.e. when the system reached the local minimum of potential energy.

In the first step, we used the "hard" collinear complex obtained in computation (5). In those calculations, the complex retained its collinear structure and sizes. The resulting position of the complex in an Ar cluster is shown in Fig. 4. The position of the nitrogen atom of the NH_2-group is close to substituted site (0,0,0). On the other side, the fluorine atom of the HF molecule occupies the nearest octahedral interstitial site O_h $(a/2, 0, 0)$, where $a = 0.54$ nm is the parameter of an Ar lattice. It happens because the distance between N and F atoms in the complex are close to one-half lattice period, $a/2$! Such commensurability leads to minor lattice distortion: two nearest argon atoms, which are placed on x-axes, and having coordinates $(a, 0, 0)$ and $(-a, 0, 0)$ shift only to $+0.003$ and -0.002 nm from the initial positions in undistorted lattice, respectively. Lattice forces affecting the complex along its C_2 axis are equal to $F_X = 6 \times 10^{-6}$ dyn. Obviously, any external forces, directed along C_2 axis of the complex, should cause its bent (out-of-plane) deformation and should lower symmetry of the complex from C_{2v} down to C_s. To determine deformations of the complex by lattice forces, we have performed computations of the complex force constants. Calculations show that the most floppy coordinates of the complex are the distance between N and H′ atoms, $R_{NH'}$, and the out-of-plane angle τ:

$$\tag{7}$$
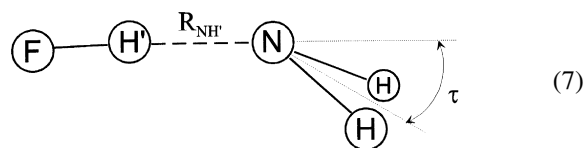
The corresponding force constants are $k_R = 2.4 \times 10^4$ dyn/cm and $k_\tau = 5.3 \times 10^3$ dyn/cm. The feasible largest deformations Δq, estimated by the simple expression $\Delta q = F_x/k_q$, are equal to $\Delta R_{NH'} = 0.003$ nm, and $\tau = 7°$. Optimisation of

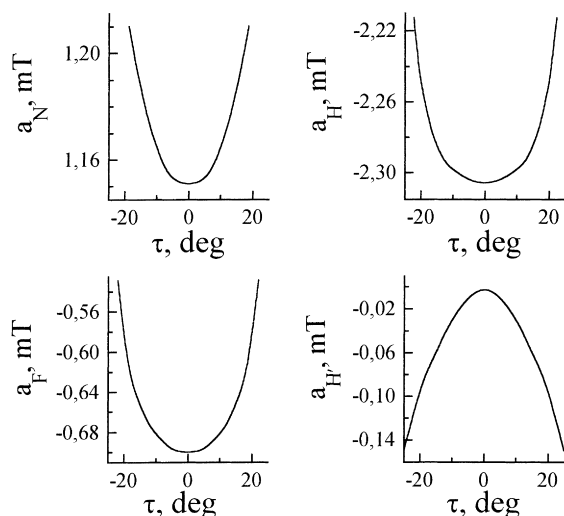Fig. 5. The calculated isotropic hyperfine constants of the NH_2–HF complex versus the out-of-plane angle τ.

such "floppy" complex in a lattice results in distortion of its geometry: $\Delta R_{NH'} = 0.001$ nm, and $\tau = 4°$.

The calculated hf constants a_N, a_H, and a_F for a distorted complex versus out-of-plane angle τ are shown in Fig. 5. As it follows from Fig. 5, the hf constants a_F and $a_{H'}$ change sharply only if τ exceeds $10°$. Moreover, if $\tau > 15°$, deviation of hf constants from their equilibrium values exceeds 0.1 mT. Based on the measured hf constants and calculated deformation τ, we may conclude that the complex suffers minor distortion in an argon lattice relative to its equilibrium geometry in a gas phase. Such minor deformations of the complex are possible, since the N and F atoms distance in the complex is close to one-half lattice parameter $a/2$. Detailed analysis of slow motion of the complex in a lattice averaging the anisotropic magnetic parameters in EPR spectra at $T > 25$ K will be given in a separate publication.

4. Conclusions

1. The radical–molecular complex NH_2–HF is observed for the first time as an intermediate product in reactions of photogenerated translationally excited and diffusing thermal F atoms with NH_3 molecules in solid argon. High yield of the complexes stabilised in an Ar matrix is provided by high binding energy in the complex.
2. EPR spectrum of NH_2–HF complex is characterised by three hyperfine splittings: triplet 1:1:1 with hf constant $a_N = 1.20$ mT, triplet 1:2:1 with $a_H = 2.40$ mT, and doublet splitting $a_F = 0.70$ mT. The hf constant at H atom of HF molecule is less than 0.05 mT.
3. The performed DFT calculation revealed that the complex NH_2–HF has a planar collinear C_{2v} structure and a binding energy of 12.3 kcal/mol. Calculated hf parameters of the complex are in good agreement with those observed in EPR experiments.
4. The complex suffers minor distortion in an argon lattice relative to its equilibrium structure in a gas phase.

References

[1] A.H. Zewail, Science 242 (1988) 1645.
[2] K. Liu, J.C. Polany, S. Yang, J. Chem. Phys. 98 (1993) 5431.
[3] E.Ya. Misochko, V.A. Benderskii, A.U. Goldschleger, A.V. Akimov, J. Am. Chem. Soc. 117 (1995) 11 997.
[4] E.Ya. Misochko, V.A. Benderskii, A.U. Goldschleger, A.V. Akimov, A.V. Benderskii, C.A. Wight, J. Chem. Phys. 106 (1997) 3146.
[5] A.U. Goldschleger, E.Ya. Misochko, A.V. Akimov, A.U. Goldschleger, V.A. Benderskii, Chem. Phys. Lett. 267 (1997) 288.
[6] J. Feld, H. Kunti, V.A. Apkarian, J. Chem. Phys. 93 (1990) 1009.
[7] E.Ya. Misochko, A.V. Akimov, C.A. Wight, Chem. Phys. Lett. 293 (1998) 547.
[8] E.Ya. Misochko, A.V. Akimov, A.U. Goldschleger, A.I. Boldyrev, C.A. Wight, J. Am. Chem. Soc. 121 (1999) 405.
[9] W.H. Duewar, D.W. Setser, J. Chem. Phys. 58 (1973) 2310.
[10] B.E. Holmes, D.W. Sester, Reaction dynamics, in: I.W.M. Smith (Ed.), Physical Chemistry of Fast Reactions, 2, Plenum Press, New York, 1979.
[11] D.J. Donaldson, J.J. Sloan, J.D. Goddard, J. Chem. Phys. 82 (1985) 4524.

[12] S. Wategaonkar, D.W. Sester, J. Chem. Phys. 86 (1987) 4477.

[13] D. Goddard, D.J. Donaldson, J.J. Sloan, Chem. Phys. 114 (1987) 321.

[14] L. Andrews, R. Lascola, J. Am. Chem. Soc. 109 (1987) 6243.

[15] E.L. Cochran, F.J. Adrian, V.A. Bowers, J. Chem. Phys. 51 (1969) 2759.

[16] M.J. Frisch, G.W. Trucks, H.B. Schlegel, P.M.W. Gill, B.G. Johnson, M.A. Robb, J.R. Cheeseman, T. Keith, G.A. Petersson, J.A. Montgomery, K. Raghavachari, M.A. Al-Laham, V.G. Zakrzewski, J.V. Ortiz, J.B. Foresman, J. Ciolowski, B.B. Stefanov, A. Nanayakkara, M. Challacombe, C.Y. Peng, P.Y. Ayala, W. Chen, M.W. Wong, J.L. Andres, E.S. Replogle, R. Gomperts, R.L. Martin, D.J. Fox, J.S. Binkley, D.J. Defrees, J. Baker, J.P. Stewart, M. Head-Gordon, C. Gonzalez, J.A. Pople, GAUSSIAN 94, Revision D.1, Gaussian Inc., Pittsburgh, PA, 1995.

[17] V. Barone, in: D.P. Chong (Ed.), Recent Advances in Density Functional Methods (Part 1), World Scientific, Singapore, 1995, p. 287.

[18] Y. Zhang, C.-Y. Zhao, X.-Z. You, J. Phys. Chem. A 101 (1997) 2879.

[19] K. Alimi, R.B. Gerber, V.A. Apkarian, J. Chem. Phys. 92 (1990) 3551.

[20] H.H. von Grünberg, H. Gabriel, Chem. Phys. Lett. 192 (1992) 503.

[21] R. Gunde, P. Felder, Hs.H. Gunthard, Chem. Phys. 64 (1982) 313.